Note

SPh functionalized bridging-vinyliminium diiron and diruthenium complexes

Luigi Busetto [a], Fabio Marchetti [b1], Rita Mazzoni [a], Mauro Salmi [a], Stefano Zacchini [a], Valerio Zanotti [a]*.

[a] *Dipartimento di Chimica Fisica e Inorganica, Università di Bologna, Viale Risorgimento 4, I-40136 Bologna, Italy*

[b] *Dipartimento di Chimica e Chimica Industriale, Università di Pisa, Via Risorgimento 35, I-56126 Pisa, Italy.*

Abstract

The –SPh functionalized vinyliminium complexes $[Fe_2\{\mu\text{-}\eta^1\text{:}\eta^3\text{-}C_\gamma(R')\text{=}C_\beta(SPh)C_\alpha\text{=}N(Me)(R)\}(\mu\text{-}CO)(CO)(Cp)_2][SO_3CF_3]$ [R = Xyl, R' = Me, **2a**; R = Me, R' = Me, **2b**; R = 4-C_6H_4OMe, R' = Me, **2c**; R = Xyl, R' = CH_2OH, **2d**; R = Me, R' = CH_2OH, **2e**; Xyl = 2,6-$Me_2C_6H_3$] are generated in high yields by treatment of the corresponding vinyliminium complexes $[Fe_2\{\mu\text{-}\eta^1\text{:}\eta^3\text{-}C_\gamma(R')\text{=}C_\beta(H)C_\alpha\text{=}N(Me)(R)\}(\mu\text{-}CO)(CO)(Cp)_2][SO_3CF_3]$ (**1a-e**) with NaH in the presence of PhSSPh. Likewise, the diruthenium complex $[Ru_2\{\mu\text{-}\eta^1\text{:}\eta^3\text{-}C_\gamma(Me)\text{=}C_\beta(SPh)C_\alpha\text{=}N(Me)(Xyl)\}(\mu\text{-}CO)(CO)(Cp)_2][SO_3CF_3]$ (**2f**) has been obtained from the corresponding vinyliminium complex $[Ru_2\{\mu\text{-}\eta^1\text{:}\eta^3\text{-}C_\gamma(Me)\text{=}C_\beta(H)C_\alpha\text{=}N(Me)(Xyl)\}(\mu\text{-}CO)(CO)(Cp)_2]$ (**1f**). The synthesis of **2c** is accompanied by formation, in comparable amounts, of the aminocarbyne complex $[Fe_2\{\mu\text{-}CN(Me)(4\text{-}C_6H_4OMe)\}(SPh)(\mu\text{-}CO)(CO)(Cp)_2]$ (**3**).

The molecular structures of **2d**, **2e** and **3** have been determined by X-ray diffraction studies.

Keywords: vinyliminium, zwitterionic complexes, disulfides, diiron complexes.

*Corresponding author. Tel.: +39 0512093695.

E-mail address: valerio.zanotti@unibo.it (V. Zanotti)

[1]Fabio Marchetti, born in 1974 in Bologna, Italy.

1. Introduction

Bridging vinyliminium complexes **1** [1] (Scheme 1) exhibit a remarkable reactivity, which results from the combination of two distinct features: the presence of an iminium group and the bridging coordination of the organic frame. Indeed, both iminium activation [2] and transformation of multisite bound organic frames [3] represent topics of current interest, for their effectiveness in providing new reactions and improved synthetic strategies. We exploited these activation effects to transform bridging vinyliminium ligands into new multifunctional coordinated species through new and unconventional reaction routes. These include proton removal from the C_β-H in the presence of 'trapping' reagents, such as diazocompounds or group 16 elements. The reactions lead to the formation of diazine-bis alkylidenes **I** [4], and zwitterionic complexes **II** [5], respectively (Scheme 1).

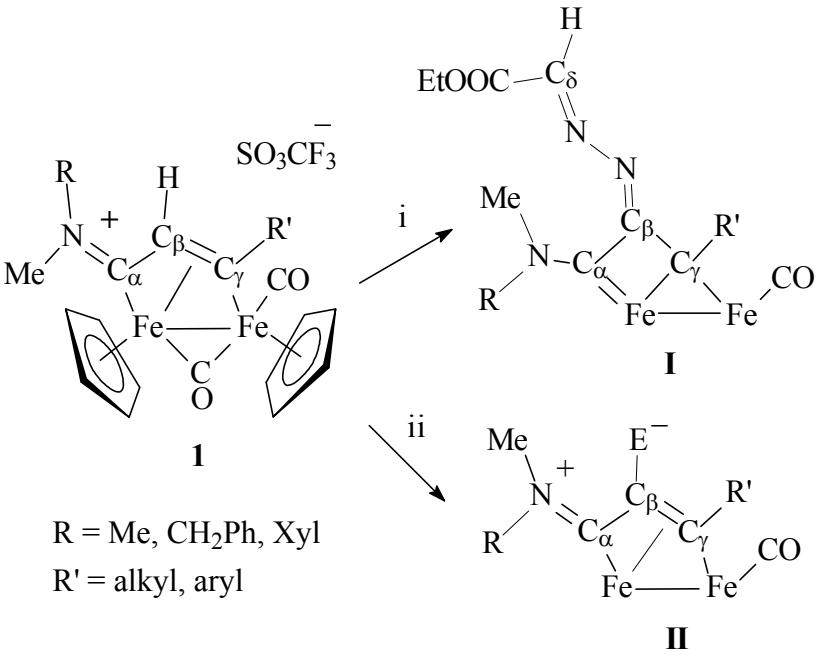

i: NaH, $N_2CH(COOEt)$; ii: NaH, E (E = O, S, Se).

Scheme 1; ancillary μ-CO and Cp ligands in **I** and **II** have been omitted for clarity.

Herein we report an extension of these studies, aimed at investigating the deprotonation of vinyliminium complexes in the presence of PhSSPh.

On the light of the influence that the substituents R and R' exert on the reactivity of the complexes **1**, a number of different vinyliminium complexes have been investigated. Likewise, the study includes a diruthenium vinyliminium complex, in order to evidence possible effects due to the nature of the metal atom.

2. Results and discussion

The vinyliminium complexes **1a-f** react with NaH, in THF at room temperature, in the presence of PhSSPh, affording the corresponding phenylthiolate vinyliminium complexes **2a-f** in about 70-80% yields (Scheme 2).

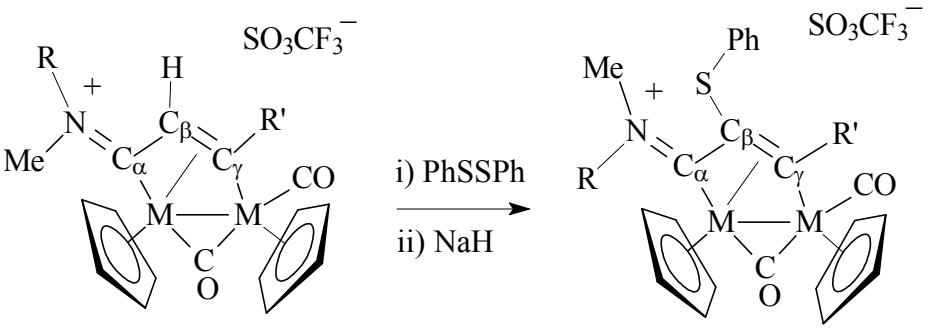

	M	R	R'	
1a	Fe	Xyl	Me	**2a**
1b	Fe	Me	Me	**2b**
1c	Fe	4-C_6H_4OMe	Me	**2c**
1d	Fe	Xyl	CH_2OH	**2d**
1e	Fe	Me	CH_2OH	**2e**
1f	Ru	Xyl	Me	**2f**

Scheme 2

Complexes **2a-f**, were purified by alumina chromatography and characterized by spectroscopy and elemental analysis. Moreover, the molecular structures of **2d** and **2e** have been ascertained by X-ray diffraction studies: the ORTEP molecular diagrams are shown in figures 1-2, whereas the most relevant bond distances and angles are reported in Table 1, where they are compared with a typical C_β substituted vinyliminium complex, *i.e. cis*-[Fe_2{μ-η^1:η^3-C_γ(Me)=C_β(Me)C_α=N(Me)(Xyl)}(μ-CO)(CO)$(Cp)_2$][SO_3CF_3] (**III**) [1b]. A hydrogen

bond exists in both structures between the C_γ-CH_2OH hydroxo group and one oxygen atom of the $[CF_3SO_3]^-$ anion [O(1)···O(10)#1 2.833(10) Å, O(1)-H(100) 0.832(11) Å, H(100)···O(10)#1 2.07(5) Å, O(1)-H(100)-O(10)#1 153(11)° for **2d**; O(1)···O(10)#1 2.861(13) Å, O(1)-H(1A) 0.81(2) Å, H(1A)···O(10)#1 2.07(3) Å, O(1)-H(1A)-O(10)#1 164(8)° and O(1)···O(30')#1 2.681(16) Å, O(1)-H(1A) 0.81(2) Å, H(1A)···O(30')#1 2.01(6) Å, O(1)-H(1A)-O(30')#1 140(8)° for **2d**]. As it can be evinced from Table 1, the bonding parameters for both **2d** and **2e** are in perfect agreement with those previously reported for other vinyliminium complexes bearing a substituent on C_β, [1b, 5, 6] confirming the usual μ-η^1:η^3-coordination to the diiron frame of the unsaturated C_3 unit. Moreover, in keeping with previous findings, the N-substituents in **2d** adopt the *Z* configuration in order to avoid steric repulsion with the –SPh group.

The overall result of the reaction shown in Scheme 1 consists in the replacement of the C_β-H hydrogen with the SPh group. It should be noted that an alternative route to the introduction of a thiolate functionality in the bridging ligand is provided by two distinct reaction steps: a) generation of the zwitterionic species **II**; b) alkylation of the S atom (Scheme 3) [6].

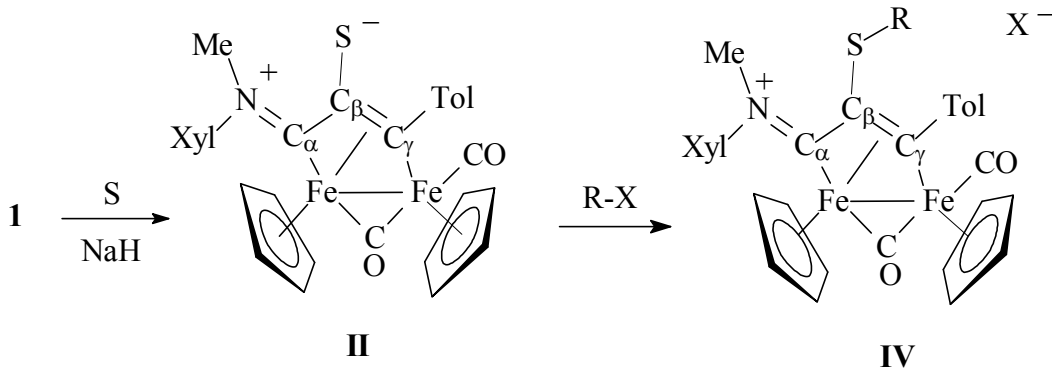

RX = $MeSO_3CF_3$, Me_3SiCl, CH_2CHCH_2I, $PhCH_2Br$.

Scheme 3

Compared to the latter procedure, the reaction with PhSSPh has the advantage of being a direct, single step synthesis, although it is limited to the introduction of the SPh functionality.

Concerning the spectroscopic properties of **2a-f**, these are consistent with the structures found in solid and very similar to those of the complexes of type **IV,** recently reported [6]. In particular, the IR spectra of **2a-f** show the usual ν-CO band pattern consisting

of two absorptions due to the terminal and bridging carbonyls (*e.g.* for **2a** at 1986 and 1826 cm^{-1}, respectively), and one additional absorption attributed to the C_α-N interaction (*e.g.* for **2a** at 1612 cm^{-1}). The NMR spectra, in $CDCl_3$ solution, reveal the presence of a single isomeric form. NOE studies carried on **2a**,**c** and **2d** indicate that the N-substituents adopt the *Z* configuration, with the steric demanding Xyl group pointing far from the C_β-substituent, as shown in solid (**2d**), and usually found in related vinyliminium complexes. It should be noted that the precursors **1a-f** display the opposite *E* configuration and, therefore, the reactions must be accompanied by inversion of configuration at the iminium moiety.

Major features in the ^{13}C NMR spectra are given by the resonances due to the C_3 bridging chain, which are similar to the corresponding values of the precursors **1a-f**. The lowfield resonances of the C_α and C_γ are consistent with their aminocarbene and bridging alkylidene character, respectively (*e.g.* for **2a** at 227.4 and 214.8 ppm). Conversely, the C_β resonance is found at *ca.* 63 ppm.

The reactions investigated included the diruthenium complex **1f**. The aim was to evidence possible effects due to the nature of the metal atom. Indeed, in a number of cases, dinuclear complexes containing ruthenium in the place of iron had shown rather different behavior [7]. However, this is not the case of **1f**, which reacts exactly as the corresponding diiron complex **1a**, and yields **2f** (Scheme 2).

All of the reactions investigated are selective, in that they afford a single product, in a single isomeric form, with one exception concerning the reaction of **1c**. In this case the synthesis of **2c** is accompanied by the formation of comparable amounts of the aminocarbyne complex $[Fe_2\{\mu\text{-}CN(Me)(4\text{-}C_6H_4OMe)\}(SPh)(\mu\text{-}CO)(CO)(Cp)_2]$ (**3**) (Scheme 4).

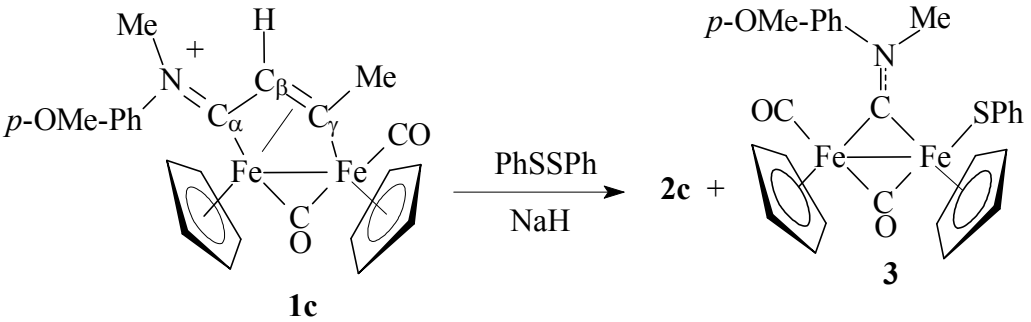

Scheme 4

Compound **3** was identified by spectroscopy and X-ray diffraction studies (Figure 3 and Table 2). The bonding parameters of **3** are in the usual ranges for this class of complexes [8] as well as the *E*-configuration of the bridging aminocarbyne ligand.

The IR spectrum of **3** shows bands due to the carbonyl ligands, at 1968 and 1789 cm^{-1}, respectively. Additional absorption at 1576 cm^{-1} accounts for the μ-CN interaction.

Bridging aminocarbyne complexes analogous to **3** usually display, in solution, two isomeric forms due to the different orientations that N substituents can assume with respect to the non-equivalent Fe atoms as a consequence of the double bond character of the μ-C-N interaction [8]. Conversely, the NMR spectra of **3** contain a single set of resonances, indicating the presence of a single isomeric form. NOE investigations did not allow to establish the orientation adopted by the *p*-$OMeC_6H_4$ and Me substituents. However, it is plausible that these are arranged according to the *E* configuration, coherently with what observed in solid. The salient feature of the ^{13}C NMR spectrum is represented by the resonance at 339.8 ppm, which accounts for the bridging aminocarbyne carbon.

The observed unique behaviour of **1c** is presumably related to the presence of the *p*-OMe-C_6H_4 substituent, although no obvious explanation can be associated. It should be remarked that the reaction formally requires alkyne (propyne) deinsertion and elimination from the bridging ligand. Indeed, a number of vinyliminium complexes, such as $[Fe_2\{\mu\text{-}\eta^1\text{:}\eta^3\text{-}C_\gamma(R')C_\beta(H)C_\alpha N(Me)R\}(\mu\text{-}CO)(CO)(Cp)_2][SO_3CF_3]$ (R = Xyl, Me; R' = Tol, $SiMe_3$), are known to undergo alkyne deinsertion, upon treatment with NaH, affording acetylide complexes of type **V** (Scheme 5) [9]. Therefore, formation of **3** might also proceed through an acetylide intermediate, which, in turn, should be transformed into the final product (Scheme 5).

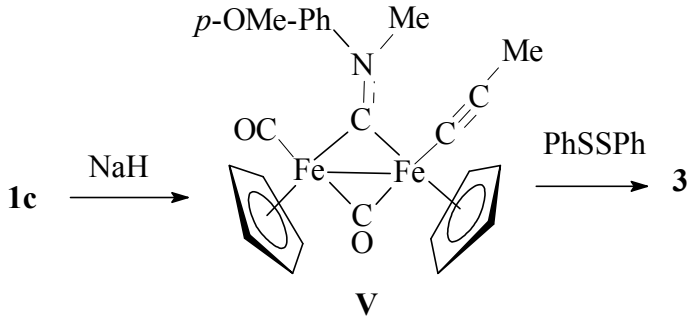

V

Scheme 5

The reactions with phenyldisulfide, with formation of **2a-f**, deserve some further comments. Most of the reactions between disulfides and metal complexes consist in the oxidative addition with S-S bond cleavage and formation of thiolate ligands. This represents a well established synthetic approach for obtaining thiolate complexes, mostly dinuclear thiolato bridged, providing an alternative and advantageous route to the use of thiolate reagents [10]. Conversely, disulfide cleavage with formation of C-S bond involving coordinated ligands is less common, in spite of the considerable interest towards metal assisted C-S bond formation [11] including, for example, the metal-catalyzed stereoselective additions of disulfides and diselenides to alkynes and olefins [12]. The formation of the complexes **1a-f** indicates that cleavage of a disulfide can be exploited to generate a C-S bond and introduce a phenyl thiolate functionality into a coordinated ligand. To the best of our knowledge, there is only one related example in which the SPh functionalization of a Cp ligand in a ferrocenyl complex, was obtained upon reaction with BuLi followed by treatment with PhSSPh [13].

A further consideration concerns the reaction mechanism. Presumably, relevant steps in the reaction sequence are the proton removal from C_β–H and the consequent reaction with PhSSPh, leading to the reductive cleavage of the S-S bond. However, alternative mechanisms based upon the homolitic cleavage of the disulfide operated by radical intermediate species should not be excluded. Indeed, radical complexes like $[Cr(CO)_3(C_5Me_5)]^{\cdot}$ are known to react with disulfides to generate thiolate derivatives $[Cr(SR)(CO)_3(C_5Me_5)]$ [14]. Likewise, the diiron thiocarbyne complex $[Fe_2(\mu\text{-}CSMe)(\mu\text{-}CO)(CO)_2(Cp)_2][SO_3CF_3]$ was described to undergo one electron reduction generating a radical which, in turn, reacted with PhSSPh affording the thiolate complex $[Fe_2(\mu\text{-}CSMe)(\mu\text{-}CO)(SPh)(CO)(Cp)_2]$ and, in minor amount, the dithiocarbene $[Fe_2\{\mu\text{-}C(SMe)(SPh)\}(\mu\text{-}CO)(CO)_2(Cp)_2]$ [15].

In order to investigate the point and provide possible clues in favor of a radical mechanism, compounds **1d-f** were treated with PhSSPh and sodium naphtalenide. The latter is a good one electron reducing agent, therefore it is expected to favor possible radical mechanisms. Unfortunately, the experiments were not conclusive: the reaction products were the same observed in the reactions with NaH, although obtained in lower yield.

The reaction between vinyliminium ligands and PhSSPh, shown in Scheme 2, is not general, in that other vinyliminium complexes, namely $[Fe_2\{\mu\text{-}\eta^1\text{:}\eta^3\text{-}$

C(R')=C(H)C=N(Me)(R)}(μ-CO)(CO)$(Cp)_2$][SO_3CF_3] (R = Xyl, R' = Tol = 4-C_6H_4Me; R = Xyl, R' = $SiMe_3$; R = Me, R' = $SiMe_3$), upon treatment with NaH in the presence of PhSSPh, failed to give the expected phenylthiolate functionalized vinyliminium complexes analogues to **2a-f**. Conversely, these reactions afforded the species which are known to be produced when the corresponding vinyliminium complexes are treated with NaH in the absence of 'trapping' reagents [9]. In other words, these vinyliminium complexes react with NaH, but the deprotonated intermediate evolve without involvement of the disulfide reagent.

3. Conclusions

In this paper we have revealed a simple, direct approach to the synthesis of phenyl thiolate functionalized vinyliminium complexes. Beside the SPh functionality, the bridging ligands display other functionalities containing heteroatoms: the NMe_2 group and, for some of the complexes, the OH group. Therefore, the bridging ligand should be exploited to coordinate further metal fragments, or to produce other transformations, which will be subject of future studies.

4. Experimental details

4.1. General

All reactions were routinely carried out under a nitrogen atmosphere, using standard Schlenk techniques. Solvents were distilled immediately before use under nitrogen from appropriate drying agents. Chromatography separations were carried out on columns of deactivated alumina (4% w/w water). Glassware was oven-dried before use. Infrared spectra were recorded at 298 K on a Perkin-Elmer Spectrum 2000 FT-IR spectrophotometer and elemental analyses were performed on a ThermoQuest Flash 1112 Series EA Instrument. ESI MS spectra were recorded on Waters Micromass ZQ 4000 with samples dissolved in CH_3CN. All NMR measurements were recorded at 298 K on Mercury Plus 400 instrument. The chemical shifts for ^1H and ^{13}C were referenced to internal TMS. The spectra were fully assigned *via* DEPT experiments and ^1H,^{13}C correlation through gs-HSQC and gs-HMBC experiments. NOE measurements were recorded using the DPFGSE-NOE sequence. All the reagents were commercial products (Aldrich) of the highest purity available and used as

received. Complexes **1a**, **1b** [1a], **1c** [4], **1d**, **1e** [1b] and **1f** [7a] were prepared as described in the literature

*4.2. Synthesis of [$M_2\{\mu$-η^1:η^3-$C_\gamma(R')=C_\beta(SPh)C_\alpha=N(Me)(R)\}(\mu$-CO)(CO)$(Cp)_2][SO_3CF_3$] [M = Fe, R = Xyl, R' = Me, **2a**; M = Fe, R = R' = Me, **2b**; M = Fe, R = 4-C_6H_4OMe, R' = Me, **2c**; M = Fe, R = Xyl, R' = CH_2OH, **2d**; M = Fe, R = Me, R' = CH_2OH, **2e**; M = Ru, R = Xyl, R' = Me, **2f**]*

To a solution of **1a** (120 mg, 0.190 mmol) in THF (10 mL) were successively added PhSSPh (205 mg, 0.939 mmol) and NaH (46 mg, 1.92 mmol). The mixture was stirred for 20 minutes and then filtered on an alumina pad. Solvent removal and chromatography of the residue on alumina, using CH_3OH as eluent, afforded **2a** as a green band. Crystallization from CH_2Cl_2 solutions layered with Et_2O, at –20 °C gave **2a** as green solid. Yield: 99 mg, 70%. Anal. Calc. for $C_{32}H_{30}F_3Fe_2NO_5S_2$: C, 51.84; H, 4.08; N, 1.89. Found: C, 51.96; H, 3.99; N, 1.99. IR (CH_2Cl_2) ν(CO) 1986 (vs), 1826 (s), ν(C_αN) 1612 (m) cm^{-1}. ^1H NMR ($CDCl_3$) δ 7.45-7.13 (8 H, Ph and $Me_2C_6H_3$); 5.62, 4.95 (s, 10 H, Cp); 4.10 (s, 3 H, C_γMe); 3.24 (s, 3 H, NMe); 2.56, 2.01 (s, 6 H, $Me_2C_6H_3$). $^{13}C\{^1H\}$ NMR ($CDCl_3$) δ 250.7 (μ-CO); 227.4 (C_α); 214.8 (C_γ); 211.0 (CO); 140.7 ($C_{ipso\ Xyl}$); 135.1 ($C_{ipso\ Ph}$); 134.0-125.5 (C_{arom}); 92.3, 89.2 (Cp); 63.0 (C_β); 49.7 (NMe); 38.8 ($C_\gamma Me$); 17.9, 17.6 ($Me_2C_6H_3$).

Compounds **2b-f** were prepared by the same procedure described for **2a**, by reacting **1b-f** with PhSSPh/NaH. Crystals of **2d** and **2e**, suitable for X-ray analyses, were collected by CH_2Cl_2 solutions layered with diethyl ether, at –20 °C.

2b (yield: 80%; colour: brown). Anal. Calc. for $C_{25}H_{24}F_3Fe_2NO_5S_2$: C, 46.10; H, 3.71; N, 2.15. Found: C, 46.16; H, 3.64; N, 2.21. IR (CH_2Cl_2) ν(CO) 1988 (vs), 1818 (s), ν(C_αN) 1671 (m) cm^{-1}. ^1H NMR ($CDCl_3$) δ 7.37-7.14 (5 H, Ph); 5.50, 4.99 (s, 10 H, Cp); 4.02 (s, 3 H, C_γMe); 3.80, 3.36 (s, 6 H, NMe). $^{13}C\{^1H\}$ NMR ($CDCl_3$) δ 251.9 (μ-CO); 223.6 (C_α); 211.0, 209.0 (CO and C_γ); 135.1 ($C_{ipso\ Ph}$); 129.8, 127.0, 126.9 (C_{arom}); 90.0, 88.4 (Cp); 63.5 (C_β); 40.0 ($C_\gamma Me$); 48.1, 44.9 (NMe).

2c (yield: 38%; colour: brown). Anal. Calc. for $C_{31}H_{28}F_3Fe_2NO_6S_2$: C, 50.09; H, 3.80; N, 1.88. Found: C, 50.00; H, 3.69; N, 1.85. IR (CH_2Cl_2) ν(CO) 1995 (vs), 1820 (s), ν(C_αN) 1636 (m) cm^{-1}. ^1H NMR ($CDCl_3$) δ 7.00, 6.80, 6.68, 6.30 (9 H, Ph and C_6H_4OMe); 5.56, 5.28 (s, 10 H, Cp); 4.33 (s, 3 H, NMe); 4.02 (s, 3 H, C_γMe); 3.52 (s, 3 H, OMe). $^{13}C\{^1H\}$ NMR

($CDCl_3$) δ 252.9 (μ-CO); 228.4 (C_α); 214.0 (C_γ); 210.7 (CO); 159.1-114.4 (C_{arom}); 92.5, 89.6 (Cp); 64.2 (C_β); 55.9 (OMe); 49.0 (NMe); 40.2 (C_γ*Me*).

2d (yield: 81%; colour: brown). Anal. Calc. for $C_{32}H_{30}F_3Fe_2NO_6S_2$: C, 50.75; H, 3.99; N, 1.85. Found: C, 50.83; H, 4.06; N, 1.84. IR (CH_2Cl_2) ν(CO) 1984 (vs), 1822 (s), ν(C_αN) 1614 (m) cm^{-1}. ^1H NMR ($CDCl_3$) δ 7.45-7.21 (8 H, Ph and $Me_2C_6H_3$); 6.72 (br, 1 H, OH); 6.21, 5.81 (dd, $^2J_{HH}$ = 14.3 Hz, $^3J_{OH}$ = 2.9 Hz, 2 H, CH_2OH); 5.61, 4.90 (s, 10 H, Cp); 3.18 (s, 3 H, NMe); 2.57, 2.02 (s, 6 H, *Me*$_2$C$_6$H$_3$). $^{13}C\{^1H\}$ NMR ($CDCl_3$) δ 251.5 (μ-CO); 226.9 (C_α); 219.2 (C_γ); 211.1 (CO); 140.6 ($C_{ipso\ Xyl}$); 135.7 ($C_{ipso\ Ph}$); 134.1-126.1 (C_{arom}); 91.6, 88.5 (Cp); 73.0 (CH_2); 62.9 (C_β); 50.0 (NMe); 18.0, 17.7 (*Me*$_2$C$_6$H$_3$).

2e (yield: 80%; colour: green). Anal. Calc. for $C_{25}H_{24}F_3Fe_2NO_6S_2$: C, 45.00; H, 3.63; N, 2.10. Found: C, 45.06; H, 3.71; N, 2.04. IR (CH_2Cl_2) ν(CO) 1991 (vs), 1815 (s), ν(C_αN) 1670 (m) cm^{-1}. ^1H NMR ($CDCl_3$) δ 7.37-7.14 (5 H, Ph); 5.91, 5.83 (dd, 2 H, $^2J_{HH}$ = 11 Hz, CH_2OH); 5.42, 5.04 (s, 10 H, Cp); 5.17 (br, 1 H, OH); 3.83, 3.41 (s, 6 H, NMe). $^{13}C\{^1H\}$ NMR ($CDCl_3$) δ 253.5 (μ-CO); 222.8 (C_α); 210.5, 209.5 (CO and C_γ); 135.6 ($C_{ipso\ Ph}$); 129.6, 127.6, 127.0 (Ph); 90.8, 88.0 (Cp); 72.9 (CH_2); 63.9 (C_β); 48.8, 45.6 (NMe).

2f (yield: 82%; colour: ochre yellow). Anal. Calc. for $C_{32}H_{30}F_3NO_5Ru_2S_2$: C, 46.20; H, 3.64; N, 1.68. Found: C, 46.22; H, 3.55; N, 1.72. IR (CH_2Cl_2) ν(CO) 1999 (vs), 1825 (s), ν(C_αN) 1634 (m) cm^{-1}. ^1H NMR ($CDCl_3$) δ 7.37-7.00 (8 H, Ph and $Me_2C_6H_3$); 5.72, 5.46 (s, 10 H, Cp); 5.52 (s, 3 H, C_γMe); 3.83 (s, 3 H, NMe); 1.93, 1.84 (s, 6 H, *Me*$_2$C$_6$H$_3$). $^{13}C\{^1H\}$ NMR ($CDCl_3$) δ 228.4 (μ-CO); 221.8 (C_α); 197.7 (CO); 184.9 (C_γ); 143.8 ($C_{ipso\ Xyl}$); 132.4-125.6 (C_{arom}); 92.4, 88.9 (Cp); 59.5 (C_β); 57.1 (C_γ*Me*); 47.1 (NMe); 17.5, 17.4 (*Me*$_2$C$_6$H$_3$).

*4.3. Synthesis of [Fe$_2${μ-CN(Me)(4-C$_6$H$_4$OMe)}(SPh)(μ-CO)(CO)(Cp)$_2$] (**3**).*

Complex **3** was obtained in the reaction of **1c** with PhSSPh/NaH, together with **2c**. Chromatography on alumina, using CH_2Cl_2 as eluent, gave **3** as second green band, which was collected and evaporated to dryness under reduced pressure. Yield: 49%. Crystals suitable for X-ray diffraction were obtained by a CH_2Cl_2 solution layered with n-pentane, at –20 °C. Anal. Calc. for $C_{27}H_{25}Fe_2NO_3S$: C, 58.40; H, 4.54; N, 2.52. Found: C, 58.36; H, 4.45; N, 2.59. IR (CH_2Cl_2) ν(CO) 1968 (vs), 1789 (s), ν(C_αN) 1576 (w) cm^{-1}. ^1H NMR ($CDCl_3$) δ 7.75-6.99 (9 H, Ph and C_6H_4OMe); 4,76, 4.68 (s, 10 H, Cp); 4.24 (s, 3 H, NMe); 3.90 (s, 3 H, OMe). $^{13}C\{^1H\}$ NMR ($CDCl_3$) δ 339.8 (μ-CN); 265.0 (μ-CO); 214.2 (CO); 158.8 ($C_{ipso\text{-}C6H4}$); 144.8-114.5 (C_{arom}); 87.4, 86.5 (Cp); 55.6 (OMe); 53.3 (NMe).

*4.4. X-ray Crystallography for **2d**, **2e** and **3·0.5Et$_2$O***

Crystal data and collection details for **2d**, **2e** and **3·0.5Et$_2$O**, are reported in Table 3. The diffraction experiments were carried out on a Bruker APEX II (for **2d** and **3·0.5Et$_2$O**) and on a Bruker AXS SMART 2000 (for **2e**) diffractometer equipped with a CCD detector using *Mo-Kα* radiation. Data were corrected for Lorentz polarization and absorption effects (empirical absorption correction SADABS) [16]. Structures were solved by direct methods and refined by full-matrix least-squares based on all data using F^2 [17]. Hydrogen atoms were fixed at calculated positions and refined by a riding model, except the O-bonded hydrogens in both **2d** and **2e** which were located in the Fourier map and refined isotropically using the 1.2 fold U_{iso} value of the parent *O*-atom. Restraints were applied to the O-H bonds (DFIX 0.83 0.01 line in SHELX). All non-hydrogen atoms were refined with anisotropic displacement parameters, unless otherwise stated. The crystals of **2d** were of very low quality and the data have been cut at low angle; even though the connectivity is certain, bond distances and angles have to be considered with care. Hydrogen bonds exist in the structures of **2d** and **2e**, between the O(1)-H groups and the oxygen atoms of the triflate anion. Similar *U* restraints were applied to the C-atoms in **2d** (s.u. 0.01) and **2e** (s.u. 0.02, only to the Cp ligands). The F- and O-atoms of the $CF_3SO_3^-$ anion (located in a general position) in **2e** are disordered; disordered atomic positions were split and refined isotropically using similar distance and similar *U* restraints and one occupancy parameter per disordered group. The Et_2O molecule in **3·0.5Et$_2$O** is disordered over two equally populated positions related by an inversion centre; in this case, an occupancy factor of 0.5 was assigned to the independent image of the moelcule and, then, refined isotropically.

Acknowledgement

We thank the Ministero dell'Università e della Ricerca Scientifica e Tecnologica (M.I.U.R.) (project: 'New strategies for the control of reactions: interactions of molecular fragments with metallic sites in unconventional species') and the University of Bologna for financial support.

Supplementary Material

Crystallographic data for the structural analyses have been deposited with the Cambridge Crystallographic Data Centre, CCDC no. 691641 for **2d**, 691639 for **2e** and 691640 for **3**. Copies of this information can be obtained free of charge from the Director, CCDC, 12 Union Road, Cambridge CB2 1EZ, UK (fax: +44-1233-336033; deposit@ccdc.cam.ac.uk or www.ccdc.cam.ac.uk).

References

[1] (a) V. G. Albano, L. Busetto, F. Marchetti, M. Monari, S. Zacchini, V. Zanotti, Organometallics 22 (2003) 1326;

(b) V. G. Albano, L. Busetto, F. Marchetti, M. Monari, S. Zacchini, V. Zanotti, J. Organomet. Chem. 689 (2004) 528.

[2] (a) A. Erkkilä, I. Majander, P. M. Pihko, Chem. Rev. 107 (2007) 5416;

(b) S. Mukherjee, J. W. Yang, S. Hoffmann, B. List, Chem. Rev. 107 (2007) 5471;

(c) B. List, Acc. Chem. Res. 37 (2004) 548;

(d) G. Lelais, D. W. C. MacMillan, Aldrichimica Acta 39 (2006) 79.

[3] (a) V. Ritleng, M. J. Chetcuti, Chem. Rev. 107 (2007) 797;

(b) M. Cowie, Can. J. Chem. 83 (2005) 1043;

(c) P. Braunstein, J. Rosé, Metal Cluster in Chemistry, P. Braunstein, L. A. Oro, P. R. Raithby Eds.; Wiley – VCH: Weinheim 1999, 616.

[4] L. Busetto, F. Marchetti, S. Zacchini, V. Zanotti, Organometallics 26 (2007) 3577.

[5] L. Busetto, F. Marchetti, S. Zacchini, V. Zanotti, Organometallics 25 (2006) 4808.

[6] L. Busetto, M. Dionisio, F. Marchetti, R. Mazzoni, M. Salmi, S. Zacchini, V. Zanotti, J. Organomet. Chem. 693 (2008) 2385.

[7] (a) L. Busetto, F. Marchetti, S. Zacchini, V. Zanotti, J. Organomet. Chem. 691 (2006) 2424;

(b) L. Busetto, F. Marchetti, S. Zacchini, V. Zanotti, Eur. J. Inorg. Chem. (2004) 1494.

[8] (a) K. Boss, M. G. Cox, C. Dowling, A. R. Manning, J. Organomet. Chem. 612 (2000) 18;

(b) K. Boss, C. Dowling, A. R. Manning, J. Organomet. Chem. 509 (1996) 197;

(c) G. Cox, C. Dowling, A. R. Manning, P. McArdle, D. Cunningham, J. Organomet. Chem. 438 (1992) 143;

(d) S. Willis, A. R. Manning, F. S. Stephens, J. Chem. Soc. Dalton Trans. 1980, 186;

(e) V. G. Albano, L. Busetto, F. Marchetti, M. Monari, V. Zanotti, J. Organomet. Chem. 649 (2002) 64;

(f) L. Busetto, F. Marchetti, S. Zacchini, V. Zanotti, Inorg. Chim. Acta 358 (2005) 1204;

(g) V. G. Albano, L. Busetto, F. Marchetti, M. Monari, S. Zacchini, V. Zanotti, Zeit. Naturf. B (2007) 427.

[9] L. Busetto, F. Marchetti, S. Zacchini, V. Zanotti, Organometallics 24 (2005) 2297.

[10] (a) E. Becker, K. Mereiter, R. Schmid, K. Kirchner, Organometallics 23 (2004) 2876;
(b) M. Md. Hossain, H.-M. Lin, J. Zhu, Z. Lin, S.-G. Shyu, Organometallics 25 (2006) 440;
(c) W.-F. Liaw, C.-H. Hsieh, S.-M. Peng, G.-H. Lee, Inorg. Chim. Acta 332 (2002) 153;
(d) C.-M. Lee, G.-Y. Lin, C.-H. Hsieh, C.-H. Hu, G.-H. Lee, S.-M. Peng, W.-F. Liaw, J. Chem. Soc., Dalton Trans. (1999) 2393;
(e) W.-F. Liaw, C.-H. Chen, G.-H. Lee, S.-M. Peng, Organometallics 17 (1998) 2370;
(f) F. Y. Petillon, P. Schollhammer, J. Talarmin, K. W. Muir, Coord. Chem. Rev. 178-180 (1998) 203;
(g) R. F. Lang, T. D. Ju, G. Kiss, C. D. Hoff, J. C. Bryan, G. J. Kubas, Inorg. Chem. 33 (1994) 3899.

[11] (a) K. Matsumoto, H. Sugiyama, J. Organomet. Chem. 689 (2004) 4564;
(b) K. Matsumoto, H. Sugiyama, Acc. Chem. Res. 35 (2002) 915.

[12] (a) I. P. Beletskaya, V. P. Ananikov, Eu. J. Org. Chem. (2007) 3431;
(b) T. Kondo, S. Uenoyama, K.Fujita, T. Mitsudo, J. Am. Chem. Soc. 121 (1999) 482.

[13] H. Seo, H. Park, B.Y. Kim, J. H. Lee, S. U. Son, Y. K. Chung, Organometallics 22 (2003) 618.

[14] T. D. Ju, K. B. Capps, R. F. Lang, G. C. Roper, C. D. Hoff, Inorg. Chem. 36 (1997) 614.

[15] N. C. Schroeder, R. J. Angelici, J. Am. Chem.Soc. 108 (1986) 3688.

[16] G. M. Sheldrick, SADABS, Program for empirical absorption correction, University of Göttingen, Germany, 1996.

[17] G. M. Sheldrick, SHELX97, Program for crystal structure determination, University of Göttingen, Germany, 1997.

Figure 1. Molecular structure of $[Fe_2\{\mu\text{-}\eta^1\text{:}\eta^3\text{-}C_\gamma(CH_2OH)=C_\beta(SPh)C_\alpha=N(Me)(Xyl)\}(\mu\text{-}CO)(CO)(Cp)_2][SO_3CF_3]$ (**2d**), with key atoms labeled (all H-atoms, except H(100), have been omitted for clarity). Thermal ellipsoids are at the 30% probability level.

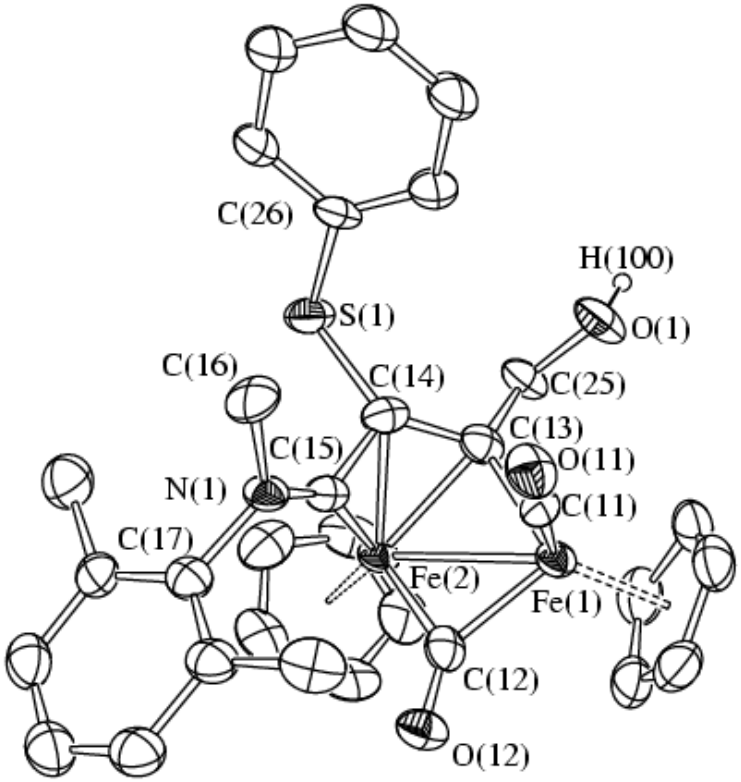

Figure 2. Molecular structure of $[Fe_2\{\mu\text{-}\eta^1\text{:}\eta^3\text{-}C_\gamma(CH_2OH)=C_\beta(SPh)C_\alpha=N(Me)_2\}(\mu\text{-}CO)(CO)(Cp)_2][SO_3CF_3]$ (**2e**) with key atoms labeled (all H-atoms, except H(1a), have been omitted for clarity). Thermal ellipsoids are at the 30% probability level.

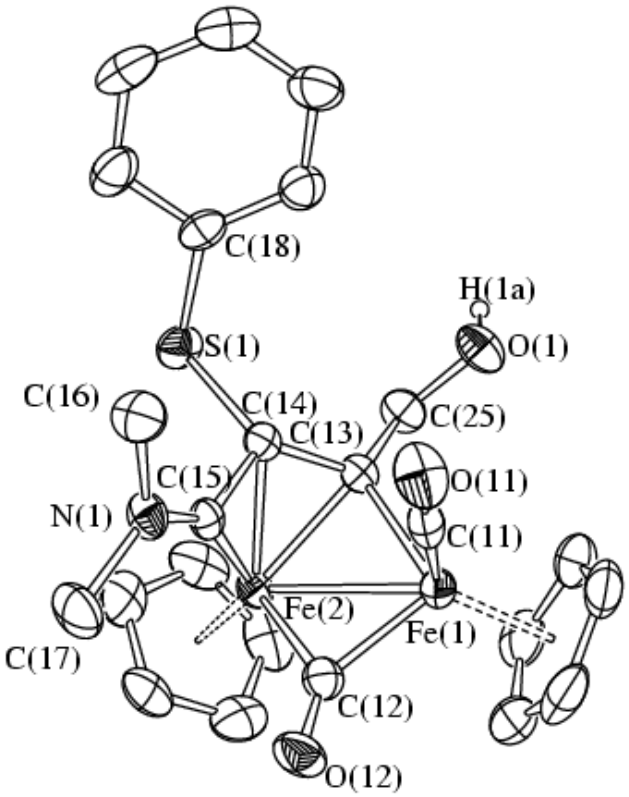

Figure 3. Molecular structure of [Fe_2{μ-CN(Me)(4-C_6H_4OMe)}(SPh)(μ-CO)(CO)$(Cp)_2$] (**3**) with key atoms labeled (all H-atoms have been omitted for clarity). Thermal ellipsoids are at the 30% probability level.

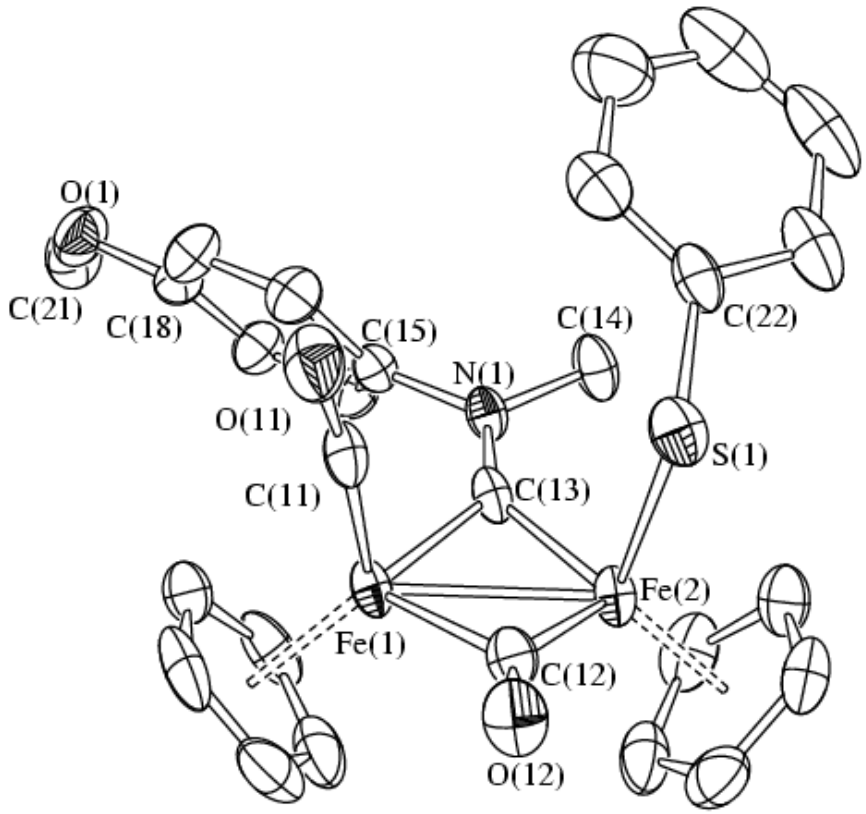

Table 1. Selected bond lengths (Å) and angles (°) for **2d** and **2e**. The most relevant bonding parameters of the C_β substituted vinyliminium complex *cis*-[$Fe_2\{\mu$-η^1:η^3-$C_\gamma(Me)=C_\beta(Me)C_\alpha$=N(Me)(Xyl)$\}(\mu$-CO)(CO)$(Cp)_2$][$SO_3CF_3$] (**III**) [1b] are reported as well for sake of comparison.

	2d	**2e**	**III**
Fe(1)-Fe(2)	2.558(2)	2.5460(11)	2.562(1)
Fe(1)-C(11)	1.742(12)	1.763(7)	1.750(9)
Fe(1)-C(12)	1.877(11)	1.891(6)	1.894(8)
Fe(2)-C(12)	1.961(11)	1.965(6)	1.944(8)
Fe(1)-C(13)	1.944(10)	1.959(5)	1.955(7)
Fe(2)-C(13)	2.051(10)	2.032(5)	2.035(7)
Fe(2)-C(14)	2.044(10)	2.034(5)	2.080(7)
Fe(2)-C(15)	1.868(12)	1.841(5)	1.839(7)
C(11)-O(11)	1.144(11)	1.134(8)	1.150(9)
C(12)-O(12)	1.195(10)	1.164(7)	1.181(9)
C(13)-C(14)	1.447(12)	1.428(8)	1.39(1)
C(14)-C(15)	1.454(13)	1.433(7)	1.43(1)
C(13)-C(25)	1.511(12)	1.509(7)	
C(25)-O(1)	1.399(10)	1.413(8)	
C(14)-S(1)	1.795(10)	1.800(5)	
C(15)-N(1)	1.279(11)	1.287(7)	1.314(8)
N(1)-C(16)	1.479(11)	1.450(8)	1.478(9)
N(1)-C(17)	1.452(12)	1.472(8)	1.454(8)
C(14)-C(13)-Fe(1)	119.0(8)	119.0(4)	121.8(5)
C(13)-C(14)-C(15)	117.4(10)	116.2(5)	155.5(6)
N(1)-C(15)-C(14)	133.4(10)	133.7(5)	131.3(7)
O(1)-C(25)-C(13)	107.5(8)	107.4(5)	
Sum angles at N(1)	359.3(16)	359.9(9)	360.0(9)

Table 2. Selected bond lengths (Å) and angles (°) for [Fe_2{μ-CN(Me)(4-C_6H_4OMe)}(SPh)(μ-CO)(CO)$(Cp)_2$] (**3**).

Fe(1)-Fe(2)	2.5081(6)	Fe(2)-S(1)	2.3101(9)
Fe(1)-C(11)	1.746(3)	C(11)-O(11)	1.148(4)
Fe(1)-C(12)	1.969(3)	C(12)-O(12)	1.182(3)
Fe(2)-C(12)	1.860(3)	C(13)-N(1)	1.303(3)
Fe(1)-C(13)	1.897(3)	Fe(2)-C(13)	1.841(3)
Fe(2)-C(12)-Fe(1)	81.78(12)	C(13)-N(1)-C(15)	123.8(2)
Fe(2)-C(13)-Fe(1)	84.28(12)	C(13)-N(1)-C(14)	122.4(3)
C(22)-S(1)-Fe(2)	111.75(10)	C(15)-N(1)-C(14)	113.7(2)

Table 3

Crystal data and experimental details for **2d[SO_3CF_3]**, **2e[SO_3CF_3]**, **3·0.5Et_2O**.

Complex	**2d**	**2e**	**3·0.5Et_2O**
Formula	$C_{32}H_{30}F_3Fe_2NO_6S_2$	$C_{25}H_{24}F_3Fe_2NO_6S_2$	$C_{29}H_{30}Fe_2NO_{3.5}S$
*F*w	757.39	667.27	592.30
T, K	293(2)	293(2)	296(2)
λ, Å	0.71073	0.71073	0.71073
Crystal system	Triclinic	Monoclinic	Monoclinic
Space group	$P\bar{1}$	$P2_1/c$	$C2/c$
a, Å	11.233(5)	10.302(2)	22.2055(14)
b, Å	11.463(5)	23.461(5)	14.0250(9)
c, Å	13.083(6)	11.478(2)	17.4654(11)
α, °	94.747(5)	90	90
β, °	98.265(6)	100.65(3)	94.6860(10)
γ, °	98.950(5)	90	90
Cell volume, Å^3	1637.3(12)	2726.3(10)	5421.1(6)
Z	2	4	8
D_c, g cm^{-3}	1.536	1.626	1.451
μ, mm^{-1}	1.075	1.279	1.180
F(000)	776	1360	2456
Crystal size, mm	0.18 × 0.16 × 0.11	0.22 × 0.15 × 0.11	0.22 × 0.16 × 0.12
θ limits, °	1.58 – 23.00	1.74 – 25.55	1.72 – 27.00
Reflections collected	8764	25188	27894
Independent reflections	4506 [R_{int} = 0.1602]	5102 [R_{int} = 0.0729]	5895 [R_{int} = 0.0454]
Data/restraints/parameters	4506 / 163 / 421	5102 / 130 / 353	5895 / 7 / 7813
Goodness on fit on F^2	0.811	1.063	1.013
R_1 [$I > 2\sigma(I)$]	0.0577	0.0647	0.0391
wR_2 (all data)	0.1237	0.1906	0.1158
Largest diff. peak and hole, e.Å^{-3}	0.322 / –-0.353	0.877 / –0.869	0.416 / –0.277

Graphical abstract

SPh functionalized bridging-vinyliminium diiron complexes

Luigi Busetto [a], Fabio Marchetti [b], Rita Mazzoni [a], Mauro Salmi [a],

Stefano Zacchini [a], Valerio Zanotti [a]*.

[a] *Dipartimento di Chimica Fisica e Inorganica, Università di Bologna, Viale Risorgimento 4, I-40136 Bologna, Italy*

[b] *Dipartimento di Chimica e Chimica Industriale, Università di Pisa, Via Risorgimento 35, I-56126 Pisa, Italy*.

SPh functionalized bridging-vinyliminium complexes **2** are conveniently obtained by reaction of the corresponding vinyliminium precursors **1** upon treatment with phenyldisulphides in the presence of NaH.

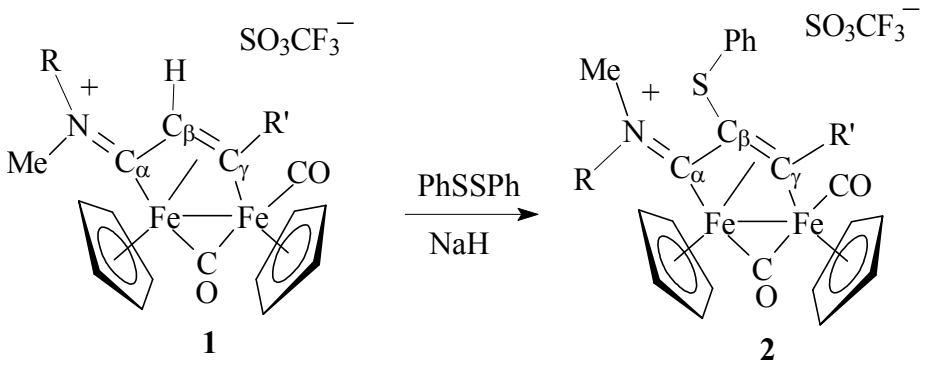

1 **2**